Elementary electronic excitations in graphene nanoribbons

L. Brey[1] and H. A. Fertig[2,3]
[1]*Instituto de Ciencia de Materiales de Madrid (CSIC), Cantoblanco, 28049 Madrid, Spain*
[2]*Department of Physics, Indiana University, Bloomington, Indiana 47405, USA*
[3]*Department of Physics, Technion, Haifa 32000, Israel*
(Received 31 January 2007; published 30 March 2007)

We analyze the collective mode spectrum of graphene nanoribbons within the random phase approximation. In the undoped case, only metallic armchair nanoribbons support a propagating plasmon mode. Landau damping of this mode is shown to be suppressed through the chirality of the single particle wave functions. We argue that undoped zigzag nanoribbons should not support plasmon excitations because of a broad continuum of particle-hole excitations associated with surface states, into which collective modes may decay. Doped nanoribbons have properties similar to those of semiconductor nanowires, including a plasmon mode dispersing as $q\sqrt{-\ln qW}$ and a static dielectric response that is divergent at $q=2k_F$.

DOI: 10.1103/PhysRevB.75.125434 PACS number(s): 73.20.Mf, 73.21.−b

I. INTRODUCTION

Recent improvements in the processing of graphite have made possible the isolation of single graphene layers.[1] These carbon sheets are very promising for microelectronic applications because they support the electric field effect: by applying a gate voltage a high mobility two-dimensional electron or hole gas can be created.[2,3] The graphene sheets could be further processed into multiterminal devices with graphene nanoribbons acting as wires connecting different nanodevices. This possibility has motivated much recent work on carbon-based nanoelectronics.

The electronic properties of graphene nanoribbons depend strongly on their size and geometry.[4,5] This dependence occurs in part because edges of the ribbons parallel to different symmetry directions require different boundary conditions. For nanoribbons with zigzag edges ("zigzag ribbons") the boundary conditions lead to a particlelike and a holelike band with evanescent wave functions confined to the surfaces,[5] which continuously evolve into the well-known zero energy surface states[6,7] as the nanoribbon width gets larger. In the case of armchair edge nanoribbons ("armchair ribbons") the band structure is metallic when the width of the sample in lattice constant units has the form $3M+1$, with M an integer, and insulating otherwise.

With respect to the lowest energy states, graphene nanoribbons are one-dimensional (1D) systems. However, their band structure is rather different than that of more conventional 1D systems. In armchair metallic nanoribbons the dispersions of the electron and hole bands are linear in momentum, whereas in armchair semiconductor nanoribbons the low energy dispersion is quadratic. On the other hand, zigzag nanoribbons have a peak in the density of states at the Fermi energy. This affects the low energy physics and the screening properties of graphene nanoribbons. In this work we compute, within the random phase approximation (RPA),[8] the dynamical polarizability and the dielectric constant of a doped graphene nanoribbon. We calculate the low energy charged collective excitations, and analyze the differences between conventional semiconductor-based one-dimensional systems and graphene nanoribbons.

We now summarize our results. Within the RPA, we find that for most undoped armchair nanoribbons there are no plasmon modes associated with interband transitions. The only exception is metallic nanoribbons, which support a plasmon that disperses as $q\sqrt{-\ln q}$, with q the momentum of the excitation along the nanoribbon. Unlike plasmons in semiconductor-based 1D systems, in metallic nanoribbons the energy of the plasmons does not depend on the level of doping of the system. The case of undoped zigzag nanoribbons turns out to be considerably more complicated, and we do not carry through a full RPA analysis as in the armchair chase. However, we argue that a broad particle-hole continuum in the zigzag case implies that any poles in the inverse dielectric function will be damped, so that there cannot be propagating plasmon modes. Finally, we show that doped semiconductor nanoribbons support low energy plasmons that disperse as $q\sqrt{-\ln q}$ and, in the armchair case, depend on the density of carriers in the ribbon in a standard way.

This paper is organized as follows. In Sec. II we introduce the Dirac Hamiltonian used for describing the electronic properties of graphene. In Secs. II A and II B we review the noninteracting electronic structure of armchair and zigzag nanoribbons. Section III is dedicated to defining a generalized dielectric function for graphene nanoribbons, and to presenting results for collective charge excitations in intrinsic (undoped) and doped graphene nanoribbons which may be derived from it. We conclude in Sec. IV with a summary of the results.

II. MODEL HAMILTONIAN

Graphene is a honeycomb structure of covalently bonded carbon atoms, which should be treated as a triangular lattice with two basis atoms, denoted by A and B, per unit cell. In graphene the low energy dispersions of the electron and hole bands are linear near the points $\mathbf{K}=\frac{2\pi}{a_0}\left(\frac{1}{3},\frac{1}{\sqrt{3}}\right)$ and $\mathbf{K}'=\frac{2\pi}{a_0}\left(-\frac{1}{3},\frac{1}{\sqrt{3}}\right)$ of the Brillouin zone. Here a_0 is the triangular lattice parameter of the graphene structure. In the $\mathbf{k}\cdot\mathbf{p}$ approximation[9,10] the wave functions are expressed in terms of envelope functions $[\psi_A(\mathbf{r}),\psi_B(\mathbf{r})]$ and $[\psi'_A(\mathbf{r}),\psi'_B(\mathbf{r})]$ for

states near the **K** and **K′** points, respectively. The envelope wave functions may be combined into a four vector which satisfies the Dirac equation $H\Psi=\varepsilon\Psi$, with

$$H=\gamma a_0\begin{pmatrix} 0 & k_x-ik_y & 0 & 0 \\ k_x+ik_y & 0 & 0 & 0 \\ 0 & 0 & 0 & -k_x-ik_y \\ 0 & 0 & -k_x+ik_y & 0 \end{pmatrix}, \quad (1)$$

where $\gamma=\sqrt{3}t/2$, with t the hopping amplitude between nearest-neighbor carbon atoms. Note that **k** denotes the separation in reciprocal space of the wave vector from the **K** (**K′**) point in the upper left (lower right) block of the Hamiltonian.

The bulk solutions of Hamiltonian (1) have energies $\varepsilon=s\gamma a_0|\mathbf{k}|$ with $s=\pm 1$ and are degenerate in the valley index. The wave functions take the form $[e^{-i\theta_{\mathbf{k}}},s,0,0]e^{i\mathbf{kr}}/C$ for the **K** valley, and $[0,0,e^{i\theta_{\mathbf{k}}},s]e^{i\mathbf{kr}}/C$ for the **K′** valley. Here $\theta_{\mathbf{k}}=\arctan k_x/k_y$, and $C=\sqrt{2L_xL_y}$ is a normalization constant, with L_x and L_y the sample dimensions.

A. Armchair nanoribbon

In an armchair nanoribbon the termination at the edges consists of a line of *A*-*B* dimers, so that the wave function amplitude should vanish on both sublattices at the extremes, $x=0$ and $x=W+a_0/2$, of the nanoribbon. To satisfy this boundary condition we must admix valleys,[5] and the confined wave functions have the form

$$\Psi_{n,s}=\frac{e^{ik_yy}}{2\sqrt{W+a_0/2}\sqrt{L_y}}\begin{pmatrix} e^{-i\theta_{k_n,k_y}}e^{ik_nx} \\ se^{ik_nx} \\ -e^{-i\theta_{k_n,k_y}}e^{-ik_nx} \\ se^{-ik_nx} \end{pmatrix} \quad (2)$$

with energies $\varepsilon_{n,s}(k_y)=sa_0\gamma\sqrt{k_n^2+k_y^2}$. The allowed values of k_n satisfy the condition[5]

$$k_n=\frac{2\pi n}{2W+a_0}+\frac{2\pi}{3a_0}. \quad (3)$$

For a width of the form $W=(3M+1)a_0$, the allowed values of k_n, $k_n=\frac{2\pi}{3a_0}\left(\frac{2M+1+n}{2M+1}\right)$, create doubly degenerate states for $n\neq -2M-1$, and allow a zero energy state when $k_y\to 0$. Nanoribbons of widths that are not of this form have nondegenerate states and do not include a zero energy mode. Thus these nanoribbons are band insulators. The allowed values of k_n are independent of the momentum k_y, and the coupling between the motion in the x and y directions only enters in the direction of the isospin of the state, θ_{k_n,k_y}.

B. Zigzag nanoribbon

The boundary conditions for zigzag nanoribbons are vanishing of the wave function on the *A* sublattice at one edge, $x=0$, and on the *B* sublattice at the other, $x=W$. The geometry of the zigzag nanoribbon does not mix the valleys, and solutions near the **K** valley with wave vector k_y are degenerate with solutions near the **K′** valley with wave vector $-k_y$.

For the **K** valley and a given value of k_y the nanoribbons wave functions take the form

$$\Psi_{n,s,k_y}=\begin{pmatrix} is\sinh(z_nx) \\ \sinh[(W-x)z_n] \end{pmatrix}\frac{e^{ik_yy}}{C}, \quad (4)$$

where C is the appropriate normalization constant. The corresponding eigenvalues are $\varepsilon=s\gamma a_0\sqrt{k_y^2-z_n^2}$ with $s=\pm 1$. The boundary conditions lead to a transcendental equation for the allowed values of z_n,

$$\frac{k_y-z_n}{k_y+z_n}=e^{-2Wz_n}. \quad (5)$$

For $k_y>1/W$, Eq. (5) has solutions with real values of z which correspond to states localized at the surface. There are two branches of such surface states, one with positive energies, and the other with negative energies. These energies approach zero as k_y increases. In undoped graphene the Fermi energy is located between these surface state branches. For $k_y<0$, there are no solutions with real z and surface states are absent. The solutions to Eq. (5) have purely imaginary z and represent confined states. For values of k_y in the range $0<k_y<1/W$, surface states from the two edges are strongly mixed and are indistinguishable from confined states. In zigzag nanoribbons the allowed values of z_n and the corresponding wave functions in the transverse direction x depend strongly on the value of the longitudinal momentum of the state k_y. This is a consequence of the chirality implicit in the Dirac Hamiltonian, Eq. (1).

III. DIELECTRIC CONSTANT

In nanoribbons the electrons are confined to move just in the y direction, and the momentum in this direction, k_y, is a good quantum number. The motion in the x direction is confined and it is described by a band index n and the conduction or valence character s. The form of the dielectric constant depends strongly on whether the motion in the longitudinal and transverse directions of the wire are coupled, as in the case of the zigzag nanoribbon, or decoupled, as in the armchair nanoribbon. In the latter case the dielectric constant can be described as a tensor in the subband indices whereas in the former case it also depends on the momentum k_y of the electronic states. For undoped ribbons, we will analyze the armchair case in detail, whereas for the zigzag case we will argue that propagating plasmons are unlikely to exist. The results for doped graphene nanoribbons are qualitatively similar to those of standard semiconductor nanowires for both cases.

A. Armchair nanoribbon

For armchair nanoribbons the motion of the carriers on the wire is coupled with the transverse motion only through the relative phases of the wave functions [cf. Eq. (2)]. In this situation the generalized dielectric function[11,12] for the nanoribbon is given by

$$\varepsilon_{ijmn}(q,\omega)=\delta_{im}\delta_{jn}-v_{ijmn}(q)\Pi_{m,n}(q,\omega), \quad (6)$$

where the function $\Pi_{mn}(q,\omega)$ is a generalized irreducible polarizability function. In this expression i,j,m,n are composite indices specifying the subband index and the valence

and/or conduction band character $s=\pm 1$. The wave vector q is along the direction in which the electron motion is free, and δ_{im} is a Kronecker delta function. The explicit expression for Π takes the form

$$\Pi_{n,n'}(q,\omega) = \frac{g_s}{L_y}\sum_{k_y} \frac{f[\epsilon_{n'}(k_y+q)] - f[\epsilon_n(k_y)]}{\epsilon_{n'}(k_y+q) - \epsilon_n(k_y) - \hbar\,\omega} \times F_{n,n'}(k_y, k_y+q), \tag{7}$$

where g_s is the spin degeneracy, $f(\epsilon)$ is the Fermi distribution function, $\epsilon_n(k_y)$ is the subband dispersion, and $F_{n,n'}(k_y, k_y+q)$ is the square of the overlap between wave functions,

$$F_{ns,n's'}(k_y, k_y+q) = \tfrac{1}{2}(1+ss'\cos\theta), \tag{8}$$

with θ the angle between the wave vectors (k_n, k_y) and $(k_{n'}, k_y+q)$. The Coulomb matrix elements for the armchair nanoribbon take the form

$$v_{ijmn}(q) = v_{|i-j|,|m-n|}(qW) = \int_0^1 du \int_0^1 du' \cos[\pi(i-j)u] \times \cos[\pi(m-n)u']v(qW|u-u'|), \tag{9}$$

where the one-dimensional Fourier transform of the Coulomb interaction has the form[13]

$$v_q(x-x') = v(q|x-x'|) = \frac{2e^2}{\epsilon_0}K_0(q|x-x'|). \tag{10}$$

Here ϵ_0 is the background dielectric constant and $K_0(x)$ is the zeroth-order modified Bessel function of the second kind, which diverges as $-\ln(x)$ when x goes to zero.

In order to obtain the last expression in Eq. (9) we have assumed that the Coulomb interaction neither produces intervalley scattering nor changes the sublattice index, as should be appropriate in the long wavelength limit. Note that the interaction is strictly zero for arbitrary q if $|i-j|+|m-n|$ is an odd integer.

In Fig. 1 we plot different matrix elements of the Coulomb interaction as a function of the momentum q. Clearly $v_{0,0}$ is much larger than the others, and it diverges as $-\ln(qW)$ when $q\to 0$. Thus, in graphene nanoribbons, both in the undoped and doped cases, the only relevant transitions at long wavelengths involve subband indices which satisfy the condition $i-j=m-n=0$. For the low energy excitations in the long wavelength limit we need only include the Coulomb matrix element $v_{0,0}$, and can to a good approximation ignore the others.

The charge density excitations are obtained by finding the zeros of the real part of the determinant of the dielectric matrix equation (6). These excitations are well-defined provided they are not damped by the continuum of electron-hole pair excitations, defined by a finite imaginary part of the determinant of the dielectric matrix.

In undoped graphene nanoribbons at zero temperature, only transitions from the valence subbands, $s=-1$ to conduction subbands, $s=1$, contribute to the polarizability. Moreover, if we include only $v_{0,0}$, the lowest energy transitions are

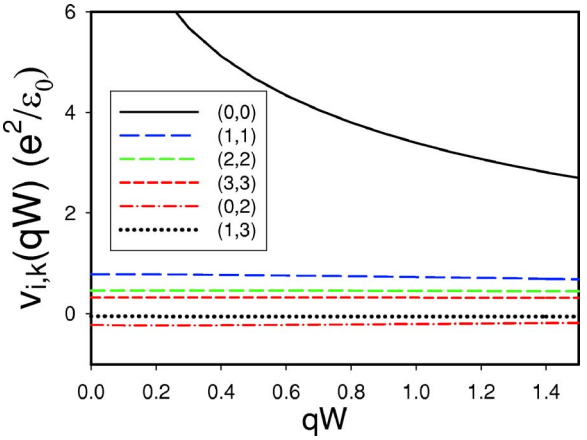

FIG. 1. (Color online) Different matrix elements of the Coulomb interaction as a function of qW for a armchair terminated nanoribbon, Eq. (9).

from the valence $(s=-1)$ to conduction $(s=1)$ bands which have the *same* subband index n. The dielectric tensor has the form

$$\varepsilon_{(n_1,s),(n_1,-s),(n_2,s'),(n_2,-s')}(q,\omega) = \delta_{ss'}\delta_{n_1,n_2} - v_{0,0}(q)\Pi_{(n_2,s'),(n_2,-s')}(q,\omega). \tag{11}$$

The zeros of the determinant of this matrix are the zeros of the function

$$1 - v_{0,0}\sum_n (\Pi_{n-,n+} + \Pi_{n+,-n-}) \equiv 1 - v_{0,0}\sum_n \chi_n, \tag{12}$$

with

$$\chi_n(q,\omega) = \frac{g_s}{L_y}\sum_{k_y} \frac{2\Delta_n(k_y,q)}{(\hbar\omega + i\delta)^2 - (\Delta_n(k_y,q))^2}F_{n-,n+}(k_y, k_y+q), \tag{13}$$

where $\Delta_n(k_y,q) = |\epsilon_n(k_y+q)| + |\epsilon_n(k_y)|$.

In Fig. 2 we show the real and imaginary parts of the dielectric constant as a function of frequency for an armchair nanoribbon of width $W=25a_0$. The lowest subband disperses linearly from zero so that the nanoribbon is metallic. Above this, the next lowest energy subband occurs for $k_1 \approx 0.13a_0^{-1}$. In Fig. 2 we see that the real part of the dielectric constant is close to unity and the imaginary part has a nonvanishing value for frequencies larger than 2 times the confinement energy of the first subband. The frequency $\tilde{\omega} = \gamma a_0(\sqrt{k_1^2+q^2}+k_1)$ defines the edge for the continuum of noninteracting intersubband electron-hole excitations. Note that the dielectric constant does not cross zero in the vicinity of these intersubband excitation energies. The absence of such zeros indicates there are no collective excitations associated with interband transitions, which in any case for energies greater than $\hbar\tilde{\omega}$ would have a finite lifetime due to Landau damping.

For much lower frequencies, the imaginary part of the dielectric function remains zero down to an energy $\sim\gamma a_0 q$, where a peak reveals the existence of electron-hole excitations at a single frequency. This corresponds to an intraband

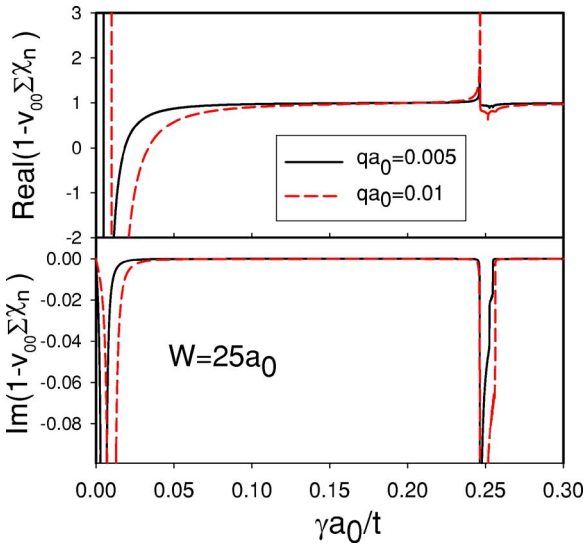

FIG. 2. (Color online) Real and imaginary part of the dielectric constant, Eq. (12), versus ω for an undoped metallic armchair nanoribbon of width $W=25a_0$. Dotted and dashed lines correspond to wave vectors $qa_0=0.005$ and $qa_0=0.01$, respectively.

excitation in the metallic subband. (We note that in the lower panel of Fig. 2 this is slightly broadened due to the small imaginary $i\delta$ added to ω to make the peak visible. In the limit $\delta\to 0$ this peak becomes a delta function.)

The collapse of the particle-hole continuum into a single line in the ω vs q plane is very common in one-dimensional metallic systems. However, its presence here turns out to depend in a fundamental way on the chirality of the Dirac fermions. This enters through the overlap F that appears in the polarizability, and guarantees that for a given q only particle-hole excitations of a single frequency contribute to Eq. (13); i.e., $\Delta_{n=0}$ is *independent* of k_y when $F\neq 0$. The overlap $F=(1+\cos\theta)/2$, with θ the angle between $(0,k_y)$ and $(0,k_y+q)$, is different than zero only for $\theta=\pi$. For excitations across the Dirac point, this corresponds to forward scattering, with a single energy for a given q. Although there is a continuum of energies for a backscattered particle, these do not contribute because the wave function overlap F strictly vanishes. This is illustrated in Fig. 3(a).

From the top panel in Fig. 2 one may see that the real part of the dielectric function vanishes at a frequency close to but just above the particle-hole excitation frequency. Since the imaginary part of the dielectric function vanishes at this frequency, one obtains a single, sharply defined plasmon mode. *This is the only collective excitation that occurs in undoped graphene nanoribbons.*

In Fig. 4 we plot the intraband plasmon frequency as a function of qW. It is clear in the figure that in the long-wavelength limit, $qW<0.001$, the Bessel function can be approximated by $-\ln(qW)$ and the plasmon disperses as $q\sqrt{-\ln(qW)}$. Keeping only intraband transitions, the effective polarizability entering in Eq. (12) for metallic armchair nanoribbons can be obtained analytically for finite temperatures and dopings,

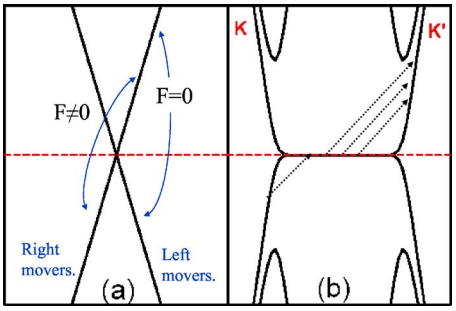

FIG. 3. (Color online) Schematic representation of the band structure and low energy electron-hole pair excitations in intrinsic (a) metallic armchair nanoribbons and (b) zigzag nanoribbons. In metallic armchair nanoribbons the chirality of the wave functions allows only transitions between carriers moving in the same direction to enter the polarizability; contributions from backscattering vanish. For a given wave vector q, because of the linear dispersion, all the electron-hole pairs entering the polarizability have the same energy $\gamma a_0 q$. In the case of zigzag nanoribbons the existence of surface states leads to a continuum in energies for electron-hole pairs with a given q.

$$\chi_0(q,\omega,\beta,\mu)=-\frac{g_s}{\pi}\frac{\gamma a_0 q}{(\hbar\omega)^2-(\gamma a_0 q)^2}f_1(q,\beta,\mu) \qquad (14)$$

with

$$f_1(q,\beta,\mu)=\frac{1}{\beta\gamma a_0}\left(-\beta\gamma a_0 q+2\ln\frac{1+e^{-\beta\mu}}{1+e^{-\beta(\gamma a_0 q+\mu)}}\right), \qquad (15)$$

with $\beta=1/k_BT$ and μ the chemical potential. This result applies both for doped and undoped nanoribbons. In the long wavelength ($q\to 0$) limit we can easily show that the plasmon frequency is given by

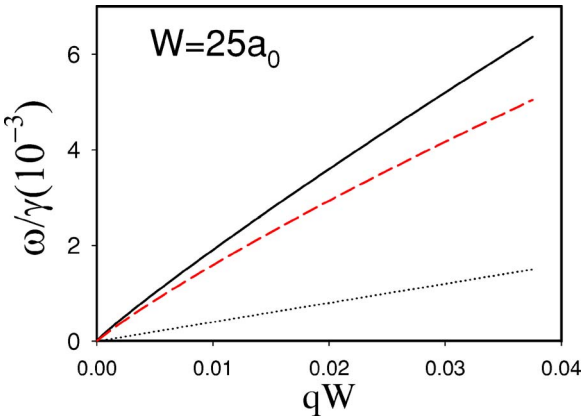

FIG. 4. (Color online) The continuous line indicates the plasmon dispersion in a metallic graphene nanoribbon calculated within the RPA. The dashed line shows the local long wavelength plasmon dispersion, Eq. (16). The dotted line is the single particle excitation.

$$\hbar\omega_p \simeq \left(\frac{2g_s e^2}{\pi\epsilon_0}\gamma a_0 q^2\right)^{1/2}\sqrt{-\ln(qW)}\sqrt{f_1(q,\beta,\mu)}. \quad (16)$$

Some comments on this result are in order. First, the plasmon has exactly the same dispersion as the normal one-dimensional plasmon of a metallic nanowire. However, at zero temperature, in graphene nanoribbons the plasmon frequency is independent of the chemical potential and therefore of the density. A classical one-dimensional plasmon has a dependence $\sqrt{n_{1D}}$, where n_{1D} is the one-dimensional carrier density. A similar anomaly occurs in two-dimensional doped graphene where the plasmon frequency behaves as $(n_{2D})^{1/4}$, compared with the $(n_{2D})^{1/2}$ classical dependence.[14–16] This anomaly in the density dependence of the plasmons is a direct consequence of the quantum relativistic nature of graphene.[16] Second, in undoped two-dimensional graphene a finite temperature produces thermoplasmon excitations associated with transitions between thermally activated electrons and holes.[17,18] In metallic nanoribbons the absence of backscattering precludes the existence of such thermoplasmon excitations. The temperature only slightly alters the plasmon dispersion. Finally, we stress the strong dependence of the plasmon dispersion on the nanoribbon width. This indicates that plasmon spectroscopy can be used as a characterization of the width of the nanoribbon.

B. Doped semiconductor armchair nanoribbon

We next analyze the low energy excitations of an electron-doped armchair nanoribbon. We confine ourselves to the case that the Fermi energy lies in the lowest energy subband. In this situation the plasmon corresponds to excitations within the same subband. The polarizability can be approximated by

$$\Pi_{0,0} = \frac{2}{\pi}\int_{-k_F}^{k_F} dk_y F_{0+,0+}(k_y,k_y+q)\frac{\Delta(k_y,q)}{(\hbar\omega)^2-\Delta(k_y,q)^2} \quad (17)$$

with $\Delta(k_y,q)=|\epsilon_1(k_y+q)|-|\epsilon_1(k_y)|$, and the collective exitations are obtained from the equation

$$1-v_{0,0}(q)\Pi_{0,0}(q,\omega)=0. \quad (18)$$

The Fermi wave vector appearing in Eq. (17) is related to the one-dimensional density of extra carriers in the nanoribbon by the expression $k_F=\pi n_{1D}/2$. In Fig. 5(b) we plot the plasmon energy for this case and for different densities. As expected in one-dimensional systems, the plasmon behaves as $q\sqrt{-\ln qW}$. However, in contrast to the metallic case, the low energy subband dispersion is parabolic, and for small q the overlap between electron and hole wave functions, $F_{0+,0+}(k_y,k_y+q)=(1+\cos\theta)/2$, is close to unity. Thus these plasmons have the usual $\sqrt{n_{1D}}$ dependence on the electron density. The possibility of backscattering is also reflected in the static polarizability. In Fig. 5(a) we plot the static polarizability as a function of the momentum. This quantity is logarithmically divergent at $q=2k_F$ as in the standard one-dimensional electron gas. This is a consequence of the perfect nesting and the possibility of backscattering from $-k_F$ to k_F. It suggests that at sufficiently low temperature, the system may be unstable to the formation of a charge density wave when coupling to lattice phonons is included.

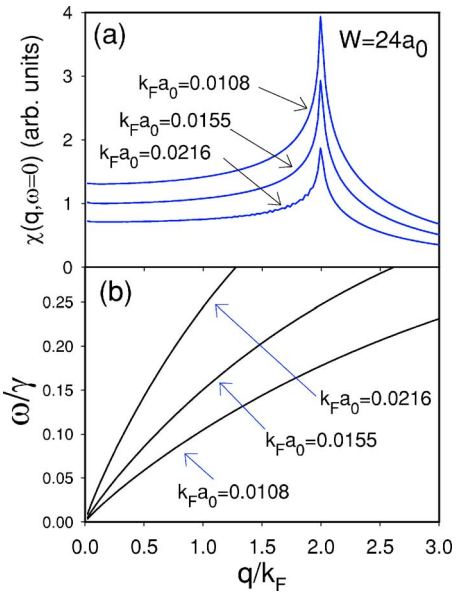

FIG. 5. (Color online) (a) The static polarizability as a function of the wave vector of a doped semiconductor armchair nanoribbon for different densities. (b) Intrasubband plasmon dispersion of the same system.

C. Zigzag nanoribbon

The calculation of plasmon poles in the zigzag nanoribbon case is complicated by the fact that the parameter z_n in the wave functions in Eq. (4) is a function of k_y. In this case the Coulomb matrix element cannot be written only as a function of the momentum transfer q. The generalized dielectric function within the RPA obeys

$$\epsilon_{ijmn}(k_y,k_y';q,\omega) = \delta_{im}\delta_{jn}\delta_{k_y,k_y'} - v_{ijmn}(k_y,k_y';q) \times g_s g_v \frac{f[\epsilon_m(k_y+q)]-f[\epsilon_n(k_y)]}{\epsilon_m(k_y+q)-\epsilon_n(k_y)-\hbar(\omega+i\delta)}. \quad (19)$$

Here $g_v=2$ is the valley degeneracy. The matrix element of the Coulomb interaction has the form

$$v_{ijmn}(k_y,k_y';q) = \int_0^W dx\int_0^W dx' \Psi^*_{i,k_y}(x)\Psi_{j,k_y+q}(x) \times v_q(x-x')\Psi^*_{m,k_y'+q}(x')\Psi_{n,k_y'}(x'), \quad (20)$$

where $\Psi^*\cdot\Psi$ denotes a dot product of the vectors appearing in Eq. (4). The collective excitation spectrum is obtained by the condition that the determinant of the dielectric matrix, Eq. (19), vanishes. In the case of undoped graphene the dielectric function is different from unity only for transitions from valence states, $s=-1$ to the conduction states $s=1$. Unlike the armchair case, in zigzag nanoribbons there is a broad particle-hole continuum of excitations, from zero energy up

to $\sim\gamma$, for small q. This occurs because of the existence of surface states which are essentially at zero energy over a broad range of k_y, allowing arbitrarily low energy particle-hole excitations for any q smaller than an appreciable fraction of the Brillouin zone size, as illustrated in Fig. 3(b). These necessarily damp any plasmon poles that might otherwise appear in the inverse dielectric function, and we expect no propagating plasmon modes for the undoped zigzag nanoribbon.

The doped case is essentially the same as that of the doped armchair nanoribbon and standard semiconducting nanowires: one may linearize the single particle spectrum around the Fermi energy, leading to a narrow line of particle-hole excitations, above which a plasmon pole should appear with dispersion $q\sqrt{-\ln qW}$.

IV. SUMMARY

In this paper we have analyzed the collective mode spectrum of graphene nanoribbons. In the undoped case, we find only metallic armchair nanoribbons support a propagating plasmon mode. This mode may propagate undamped because the chirality of the wave functions prevents it from decaying into particle-hole pairs. We argued that undoped zigzag nanoribbons will not support plasmon excitations because this supports a broad continuum of particle-hole excitations with low wave vectors, and there is nothing to protect a plasmon from decaying into this. Doped nanoribbons turn out to have properties similar to those of semiconductor nanowires, including a plasmon mode dispersing as $q\sqrt{-\ln qW}$ with a coefficient that vanishes when the doping vanishes (except in the metallic armchair case), and a static dielectric response that is divergent at $q=2k_F$.

ACKNOWLEDGMENTS

The authors thank P. de Andrés, F.Guinea and P. López-Sancho for helpful discussions. One of the authors (L.B.) was supported by MAT2006-03741 (Spain) and one of the authors (H.A.F.) was supported by NSF through Grant No. DMR-0454699. The authors also thank the KITP Santa Barbara (NSF Grant No. PHY05-51164) where this work was finished.

[1] K. S. Novoselov, A. K. Geim, S. V. Mozorov, D. Jiang, Y. Zhang, S. V. Dubonos, I. V. Gregorieva, and A. A. Firsov, Science **306**, 666 (2004).
[2] K. S. Novoselov, A. K. Geim, S. V. Mozorov, D. Jiang, M. I. V. Gregorieva, S. V. Dubonos, and A. A. Firsov, Nature (London) **438**, 197 (2005).
[3] Y. Zhang, Y.-W. Tan, H. L. Stormer, and P. Kim, Nature (London) **438**, 201 (2005).
[4] M. Ezawa, Phys. Rev. B **73**, 045432 (2006).
[5] L. Brey and H. A. Fertig, Phys. Rev. B **73**, 235411 (2006).
[6] M. Fujita, K. Wakabayashi, K. Nakada, and K. Kusakabe, J. Phys. Soc. Jpn. **65**, 1920 (1996).
[7] N. M. R. Peres, F. Guinea, and A. H. Castro Neto, Phys. Rev. B **73**, 125411 (2006).
[8] G. D. Mahan, *Many-Particle Physics*, 3rd ed. (Kluwer Academic, New York, 2000).
[9] T. Ando, J. Phys. Soc. Jpn. **74**, 777 (2005).
[10] D. P. DiVincenzo and E. J. Mele, Phys. Rev. B **29**, 1685 (1984).
[11] Q. Li and S. Das Sarma, Phys. Rev. B **40**, 5860 (1989).
[12] S. Das Sarma, Phys. Rev. B **29**, 2334 (1984).
[13] Q. P. Li and S. Das Sarma, Phys. Rev. B **43**, 11768 (1991).
[14] T. Ando, J. Phys. Soc. Jpn. **75**, 074716 (2006).
[15] B. Wunsch, T. Stauber, F. Sols, and F. Guinea, New J. Phys. **8**, 318 (2006).
[16] E. H. Hwang and S. Sarma, cond-mat/0610561 (to be published).
[17] O. Vafek, Phys. Rev. Lett. **97**, 266406 (2006).
[18] V. Apalkov, X.-F.Wang, and T. Chakraborty, cond-mat/0611465 (to be published).